the initial position (i.e., scission point) distribution from the experimental angular distribution. This fact was used in the determination of the initial distribution in Sec. V. In the same fashion, we obtained the average emission point $\bar{X}_0$ as a function of R from the experimental angular distributions for various values of R which were shown in Fig. 10 of the preceding paper. For the three-point-charge model $\bar{X}_0$ varies from 10×10^{-13} cm from the center of the heavy fragment (for $R=1$) to 11×10^{-13} cm from the center of the light fragment (for $R=2$). While these values of $\bar{X}_0$ may be substantially different for the physical scissioning nucleus, our calculation nevertheless supports the view expressed in the above-mentioned paper that the scission point moves closer *to the light fragment as R increases*, and that the variation in $\bar{X}_0$ as a function of R amounts to a substantial part of the distance between the centers of the fragment at the moment of scission.

We have presented additional support for the argument first given by Halpern[3,5] that, at the moment of scission, the fragments have already acquired a substantial part of their kinetic energy. Our calculation shows that good agreement with the experimental results is obtained if we assume that the average energy of the α particle at the moment of scission is $\bar{E}_{\alpha 0}\simeq3$ MeV, the average total kinetic energy of the two fragments is $\bar{E}_{F0}\simeq40$ MeV, and the average distance between the centers of the two fragments is $\bar{D}\simeq26\times10^{-13}$ cm. These conclusions contradict the assumption of the statistical theory of fission[4] that at the moment of scission the kinetic energy of the two fragments is negligible (less than 1.0 MeV). It may of course be argued that our conclusions pertain only to LRA fission and that in binary fission the scission moment occurs much earlier, when the kinetic energy of the fission fragments is indeed still negligible. Such a situation is unlikely in view of the great similarity of the two processes, as seen in the preceding paper. It would leave unexplained the fact that LRA fission is also asymmetric.

ACKNOWLEDGMENTS

The authors would like to thank L. Meilen and M. Weinstein for their help in the computations. They would also like to thank Dr. J. R. Nix for many valuable comments.

PHYSICAL REVIEW VOLUME 156, NUMBER 4 20 APRIL 1967

(d,p) and (d,t) Reactions on the Isotopes of Tin*

EDWARD J. SCHNEID,† ANAND PRAKASH,‡ AND BERNARD L. COHEN
University of Pittsburgh, Pittsburgh, Pennsylvania

(Received 15 March 1965; revised manuscript received 28 November 1966)

Energy levels up to ~4-MeV excitation energy are studied using the (d,p) and (d,t) reactions. Spectroscopic factors for most of the levels are obtained with the aid of distorted-wave Born-approximation (DWBA) calculations. The $\frac{7}{2}^+$ state is not identified in Sn^{123} and Sn^{125}. Several new $l=2$ states are identified as well as several $l=1$ and $l=3$ states belonging to the 82–126-neutron shell. A renormalization of the DWBA absolute cross sections is performed to eliminate systematic inconsistencies in the sum of $U_j^2+V_j^2$. The factors of renormalization are found to be within the well-known uncertainties of the DWBA calculations. The values of relative single-particle energies $(\epsilon_j-\epsilon_{5/2})$ are calculated both from the occupation numbers (U_j^2 or V_j^2) and from the single-quasiparticle energies (E_j) using pairing theory. The results are in disagreement by as much as 1 MeV or more. From the reactions on the odd isotopes, spin and parity information is obtained for many states in Sn^{114}, Sn^{116}, Sn^{118}, and Sn^{120}.

I. INTRODUCTION

THE (d,p) and (d,t) "stripping" reactions have been found to be very useful for shell-model studies of nuclear structure. The excitation energies and transition strengths of the nuclear levels excited in these reactions yield direct information about the excitation energies and the occupation numbers of the single-particle shell-model states.

The tin isotopes are particularly well suited to provide information about the 50–82-neutron shell. In tin, the protons form a closed shell ($Z=50$), making the neutron spectrum relatively simple. The large number of stable isotopes also provide many targets, so trends can be observed as the neutron shell is filling.

In a previous work,[1] the nuclear structure of the tin isotopes was investigated. The work reported here represents an improvement over that study in that: (1) thinner targets have been obtained[2] which allows a

Work performed at the Sarah Mellon Scaife Radiation Laboratory and supported by the National Science Foundation.

† Present address: Rutgers, The State University, New Brunswick, New Jersey.

‡ Present address: Yale University, New Haven, Connecticut.

[1] B. L. Cohen and R. E. Price, Phys. Rev. **121**, 1441 (1961).

[2] The tin isotopes as self-supporting foils were obtained from the stable Isotopes Division, Oak Ridge National Laboratory, Oak Ridge, Tennessee.

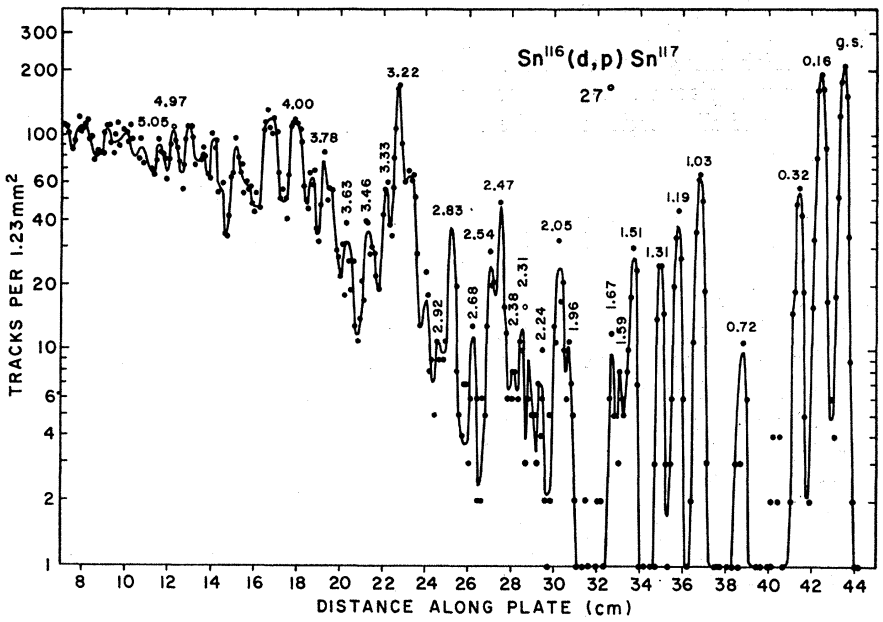

FIG. 1. Measured proton energy spectrum from $Sn^{116}(d,p)Sn^{117}$. The excitation energies in MeV for the levels in Sn^{117} are indicated above the peaks. The energy resolution is typical for the data.

factor of 2 improvement in the energy resolution; (2) targets of the rare, light isotopes of mass numbers 112, 114, and 115 have been obtained, so that the data can be extended to this mass region[3]; distorted-wave Born-approximation (DWBA) calculations have become available for use in the analysis; and (4) the energy calibration of the magnetic spectrograph has been improved, allowing more accurate energy determinations.

II. EXPERIMENTAL

The experimental method has been described in detail in an earlier paper.[3] The targets were bombarded with 15-MeV deuterons from the University of Pittsburgh 47-in. fixed frequency cyclotron. The reaction products were analyzed by a 60° wedge magnet spectrograph and detected with nuclear emulsion plates. The thicknesses of the targets were between 2 and 4 mg/cm^2; they were measured with an accuracy of 10% or better. The energy resolution obtained in this study varied from approximately 40 keV at favorable angles for the thinner targets to about 60 keV at less favorable angles for the thicker targets.

For the (d,p) analysis, data were obtained at eight angles: 9, 12, 18, 21, 27, 31, 40, and 50 deg. These key angles were judiciously chosen in order to determine the values of orbital angular momentum transfer l_n. In the (d,t) analysis, data were obtained at only two angles, 45 and 60 deg. Typical (d,p) and (d,t) spectra are shown in Figs. 1 and 2.

For the (d,t) reaction, the states of high excitation energies were not studied, since in magnetic analysis of the reaction products, deuterons from elastic and inelastic scattering are focused into the region where the triton energy is less than 10 MeV. Thus, the triton data are limited to energies above 10 MeV. In most cases, however, a sufficient range of triton energies was available for the states of the 50–82-neutron shell to be observed. No data were obtained from the $Sn^{112}(d,t)$ reaction

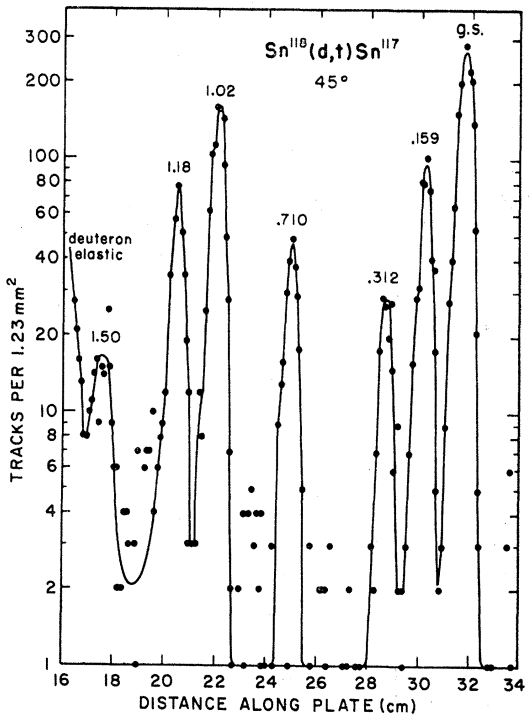

FIG. 2. Measured triton energy spectrum from $Sn^{118}(d,t)Sn^{117}$. The excitation energies in MeV for the levels in Sn^{117} are indicated above the peaks.

[3] B. L. Cohen, R. H. Fulmer, and A. L. McCarthy, Phys. Rev. **126**, 689 (1962).

because of the large negative Q value for this reaction. In measurements of the protons from (d,p) reactions, an absorber thick enough to stop deuterons, tritons, and α particles was placed over the nuclear emulsions, so that protons of all energies could be observed without interference.

III. RESULTS OF THE (d,p) AND (d,t) REACTIONS ON EVEN TARGETS

The experimental results for the (d,p) and (d,t) reaction on the even mass isotopes of tin are summarized in Tables I–VII, respectively. These tables list the energies of the observed nuclear levels, the assigned values of orbital angular momentum transfer l_n, the assigned final spins of these states, the (d,p) absolute cross section evaluated at the maximum in the angular distribution (beyond 9°), the spectroscopic factor determined by the (d,p) reaction, and the (d,t) absolute cross section observed at 45°. The quantities which are listed in parentheses are only tentatively assigned values. The spectroscopic factor S for the (d,p) reactions is determined using the relation

$$\frac{d\sigma}{d\Omega}=\frac{2J+1}{2I+1}\sigma(l,\theta,Q)S, \tag{1}$$

where $d\sigma/d\Omega$ is the experimental absolute differential cross section, J is the spin of state observed in the stripping process, I is the spin of the target nucleus (zero for even-even targets), and $\sigma(l,\theta,Q)$ is the single-particle

TABLE I. The energy levels of Sn^{113} from the (d,p) and (d,t) reactions. Listed are the energies, the values of angular momentum transfer, the assigned spins and parity, the absolute cross section for (d,p) taken at the first maximum beyong 9°, the spectroscopic factors and the absolute cross section for (d,t) taken at 45°.

E^* (MeV)	(d,p) l_n	J^π	$(d\sigma/d\Omega)_{max}$ (mb/sr)	$S_{d,p}$	(d,t) E	$d\sigma/d\Omega(45°)$ (mb/sr)
0	0	$\frac{1}{2}^+$	4.23	1.16	0	0.699
0.07	4	$\frac{7}{2}^+$	0.263	0.31	0.07	0.371
0.41	2	$\frac{5}{2}^+$	1.76	0.15	0.39	1.304
0.50	2	$\frac{3}{2}^+$	4.75	0.75	0.49	0.314
0.74	5	$11/2^-$	1.20	1.30		
1.01	2	$(\frac{5}{2}^+)$	0.216	0.017		
1.56	2	$(\frac{5}{2}^+)$	0.730	0.053		
1.82	0	$\frac{1}{2}^+$	0.423	0.090		
1.94	1	$(\frac{3}{2}^-)$	0.222	0.011		
2.12	3	$(\frac{7}{2}^-)$	0.437	0.056		
2.29	3	$(\frac{7}{2}^-)$	0.332	0.041		
2.53	3	$(\frac{7}{2}^-)$	0.460	0.055		
2.61	3	$(\frac{7}{2}^-)$	0.397	0.047		
2.77	3	$(\frac{7}{2}^-)$	0.326	0.037		
2.86	3	$(\frac{7}{2}^-)$	0.676	0.078		
2.98	3	$(\frac{7}{2}^-)$	0.344	0.038		

TABLE II. Energy levels of Sn^{116} from the (d,p) and (d,t) reactions. (See also caption for Table I.)

E^* (MeV)	(d,p) l_n	J^π	$(d\sigma/d\Omega)_{max}$ (mb/sr)	$S_{d,p}$	(d,t) E^* (MeV)	$d\sigma/d\Omega(45°)$ (mb/sr)
0	0	$\frac{1}{2}^+$	3.67	0.960	0	1.61
0.49	2	$\frac{3}{2}^+$	3.96	0.62	0.48	0.314
0.60	4	$\frac{7}{2}^+$	0.209	0.19	0.61	0.368
0.73	5	$\frac{11}{2}^-$	0.741	0.77	0.72	0.112
0.98	2	$\frac{5}{2}^+$	1.52	0.12	0.98	1.43
1.28	2	$(\frac{5}{2}^+)$	0.40	0.029	1.25	0.053
					1.30	0.080
1.63	(2)	$(\frac{5}{2}^+)$	0.63	0.044		
1.97	(0)	$\frac{1}{2}^+$	0.41	0.082		
2.07	(0)	$\frac{1}{2}^+$	0.23	0.045		
2.17	(2)	$(\frac{5}{2}^+)$	0.33	0.021		
2.49	(2)	$(\frac{5}{2}^+)$	0.35	0.021		
2.77	(1)	$(\frac{3}{2}^-)$	0.89	0.050		
2.95	(3)	$(\frac{7}{2}^-)$	0.56	0.064		
3.05	(3)	$(\frac{7}{2}^-)$	0.62	0.061		
3.18	(3)	$(\frac{7}{2}^-)$	0.82	0.070		
3.82	(3)	$(\frac{7}{2}^-)$	0.79	0.080		
3.67	(3)	$(\frac{7}{2}^-)$	0.70	0.065		
3.83			0.84			

TABLE III. The energy levels of Sn^{117} from the (d,p) and (d,t) reactions. (See also caption for Table I.)

E^* (MeV)	(d,p) l_n	J^π	$(d\sigma/d\Omega)_{max}$ (mb/sr)	$S_{d,p}$	(d,t) E^* (MeV)	$d\sigma/d\Omega(45°)$ (mb/sr)
0	0	$\frac{1}{2}^+$	2.74	0.65	0	2.26
0.16	2	$\frac{3}{2}^+$	3.72	0.55	0.16	0.695
0.32	5	$11/2^-$	0.800	0.81	0.31	0.212
0.72	4	$\frac{7}{2}^+$	0.166	0.13	0.71	0.306
1.03	2	$\frac{5}{2}^+$	0.875	0.061	1.01	1.15
1.19	2	$\frac{5}{2}^+$	0.490	0.033	1.18	0.526
1.31	(3)	$(\frac{7}{2}^-)$	0.226	0.029		
1.51	(2)	$(\frac{5}{2}^+)$	0.315	0.020	1.50	0.173
1.59	(2)	$(\frac{5}{2}^+)$	0.098	0.006		
1.67	(2)	$(\frac{5}{2}^+)$	0.106	0.007		
1.96	(1+3)	$(\frac{3}{2}^-)$	0.040	0.003		
		$(\frac{7}{2}^-)$	0.020	0.002		
2.05	(3)	$(\frac{7}{2}^-)$	0.277	0.025		
2.24	...	...	...	...		
2.31	(2)	$(\frac{5}{2}^+)$	0.205	0.012		
2.38	...	...	...	...		
2.47	(3)	$(\frac{7}{2}^-)$	0.293	0.030		
2.54	(3)	$(\frac{7}{2}^-)$	0.167	0.017		
2.68	(3)	$(\frac{7}{2}^-)$	0.134	0.013		
2.83	...	...	...	...		
2.92	(1)	$(\frac{3}{2}^-)$	1.076	0.058		
3.22	(3)	$(\frac{7}{2}^-)$	1.413	0.120		
3.33	(1)	$(\frac{3}{2}^-)$	0.538	0.030		
3.46	(1)	$(\frac{3}{2}^-)$	1.41	0.079		
3.63	(1)	$(\frac{3}{2}^-)$	0.682	0.039		
3.78	(3)	$(\frac{7}{2}^-)$	0.410	0.030		
4.00			1.82			
4.97	(1)	$(\frac{3}{2}^-)$	2.2	0.14		
5.05			0.743			

TABLE IV. The energy levels of Sn^{119} from the (d,p) and (d,t) reactions. (See also caption for Table I.)

E^* (MeV)	(d,p) l_n	(d,p) J^π	$(d\sigma/d\Omega)_{max}$ (mb/sr)	$S_{d,p}$	(d,t) E^* (MeV)	(d,t) $d\sigma/d\Omega(45°)$ (mb/sr)
0	0	$\frac{1}{2}^+$	2.70	0.59	0	
0.024	2	$\frac{3}{2}^+$	3.63	0.52	0.030	
0.08	5	$11/2^-$	0.522	0.56	0.08	
0.79	4	$\frac{7}{2}^+$	0.183	0.14	0.78	0.304
0.93	2	$\frac{5}{2}^+$	0.085	0.006	0.92	0.146
1.10	2	$\frac{5}{2}^+$	1.29	0.084	1.08	1.32
1.22	2	$\frac{5}{2}^+$	0.127	0.008	1.24	0.055
1.37	2	$\frac{5}{2}^+$	0.216	0.014	1.36	0.356
1.59	2	$\frac{5}{2}^+$	0.114	0.007	1.56	0.060
					1.64	0.031
1.74	2	$\frac{5}{2}^+$	0.209	0.011	1.73	0.085
1.95	(1)	$\frac{3}{2}^-$	0.214	0.011		
2.58	(2+1)	$(\frac{5}{2}^+)$	0.49	0.025		
		$(\frac{3}{2}^-)$	0.360	0.014		
2.68	(3)	$(\frac{7}{2}^-)$	1.25	0.12		
2.92	(1)	$(\frac{3}{2}^-)$	1.02	0.057		
3.13	(1)	$(\frac{3}{2}^-)$	0.070	0.046		
3.23	(3)	$(\frac{7}{2}^-)$	0.745	0.089		
3.33	(3)	$(\frac{7}{2}^-)$	0.483	0.037		
3.54	(3)	$(\frac{7}{2}^-)$	1.19	0.086		
3.67	(3)	$(\frac{7}{2}^-)$	1.68	0.118		
3.87	(3)	$(\frac{7}{2}^-)$	2.18	0.146		

TABLE V. Energy levels of Sn^{121} from the (d,p) and (d,t) reactions. (See also caption for Table I.)

E^* (MeV)	(d,p) l_n	(d,p) J^π	$(d\sigma/d\Omega)_{max}$ (mb/sr)	$S_{d,p}$	(d,t) E^* (MeV)	(d,t) $d\sigma/d\Omega(45°)$ (mb/sr)
0	2	$\frac{3}{2}^+$	3.17	0.43	0	1.45
0.05	0	$\frac{1}{2}^+$	1.93	0.39	0.056	3.09
0.05	5	$11/2^-$	0.235	0.21	0.05	
0.93	4	$\frac{7}{2}^+$	0.276	0.19	0.90	0.381
1.12	2	$\frac{5}{2}^+$	1.03	0.065	1.11	1.47
1.40	2	$\frac{5}{2}^+$	0.477	0.029	1.37	0.802
1.71	2	$(\frac{5}{2}^+)$	0.082	0.004		
1.91	(1)	$(\frac{3}{2}^-)$	0.125	0.007		
2.06	(3)	$(\frac{7}{2}^-)$	0.047	0.005		
2.25	(2)	$(\frac{5}{2}^+)$	0.503	0.027		
2.45	(3)	$(\frac{7}{2}^-)$	0.234	0.021		
2.59	(3)	$(\frac{7}{2}^-)$	0.405	0.035		
2.69	(3)	$(\frac{7}{2}^-)$	2.24	0.185		
2.93			0.432			
3.10	(1)	$(\frac{3}{2}^-)$	2.01	0.13		
3.37	(1)	$(\frac{3}{2}^-)$	1.32	0.077		
3.51	(1)	$(\frac{3}{2}^-)$	2.44	0.15		
3.69	(1)	$(\frac{3}{2}^-)$	2.24	0.14		
3.85	(1)	$(\frac{3}{2}^-)$	0.600	0.037		
3.93	(1)	$(\frac{3}{2}^-)$	1.53	0.095		
4.16	(1)	$(\frac{3}{2}^-)$	1.14	0.073		
4.25	(1)	$(\frac{3}{2}^-)$	0.830	0.053		

TABLE VI. Energy levels of Sn^{123} from the (d,p) and (d,t) reactions. (See also caption for Table I.)

E^* (MeV)	(d,p) l_n	(d,p) J^π	$(d\sigma/d\Omega)_{max}$ (mb/sr)	$S_{d,p}$	(d,t) E^* (MeV)	(d,t) $d\sigma/d\Omega(45°)$ (mb/sr)
0	5	$11/2^-$	···	···	0	
0.02	2	$\frac{3}{2}^+$	3.32	0.43	0.02	2.21
0.15	0	$\frac{1}{2}^+$	1.91	0.36	0.15	3.79
0.94	···	···	0.226	···	0.91	0.048
1.20	2	$\frac{5}{2}^+$	1.02	0.062	1.17	1.930
1.49	2	$\frac{5}{2}^+$	0.467	0.024	1.48	1.006
1.83	(1)	$(\frac{3}{2}^-)$	0.034	0.003		
1.92	(2)	$(\frac{5}{2}^+)$	0.037	0.002		
2.16	(1+2)	$\frac{3}{2}^-$	0.030	0.002		
		$(\frac{5}{2}^+)$	0.050	0.004		
2.29	(1)	$(\frac{3}{2}^-)$	0.058	0.005		
2.40	(0)	$(\frac{1}{2}^+)$	0.072	0.012		
2.73			3.78			
2.83	(3)	$(\frac{7}{2}^-)$	0.282	0.023		
3.07	(3)	$(\frac{7}{2}^-)$	0.503	0.036		
3.14	(3)	$(\frac{7}{2}^-)$	1.61	0.12		
3.40	(1)	$(\frac{3}{2}^-)$	3.20	0.23		
3.53	(1)	$(\frac{3}{2}^-)$	0.595	0.043		
3.73			1.20			
3.81	(1)	$(\frac{3}{2}^-)$	2.06	0.14		
4.05	(1)	$(\frac{3}{2}^-)$	1.62	0.11		
4.25			1.75			
4.45			0.913			

TABLE VII. Energy levels of Sn^{125} from the (d,p) reaction. (See also caption for Table I.)

E^* (MeV)	l_n	J^π	$(d\sigma/d\Omega)_{max}$	$S_{d,p}$
0	5	$11/2^-$	···	···
0.026	2	$\frac{3}{2}^+$	2.69	0.34
0.22	0	$\frac{1}{2}^+$	1.44	0.25
0.94	···	···	0.145	···
1.27	(2)	$(\frac{5}{2}^+)$	0.621	0.039
1.56	(2)	$(\frac{5}{2}^+)$	0.400	0.023
1.78	···	···	0.03	···
2.27	(0)	$\frac{1}{2}^+$	0.054	0.009
2.35	(1)	$(\frac{3}{2}^-)$	0.081	0.007
2.59	(3)	$(\frac{7}{2}^-)$	0.136	0.011
2.76			7.20	
3.00			0.400	
3.07	(1)	$(\frac{3}{2}^-)$	0.496	0.036
3.18	(3)	$(\frac{7}{2}^-)$	0.880	0.058
3.35	(3)	$(\frac{7}{2}^-)$	0.988	0.062
3.42	(1)	$(\frac{3}{2}^-)$	4.79	0.34
3.53	(1)	$(\frac{3}{2}^-)$	0.608	0.042
3.63	(3)	$(\frac{7}{2}^-)$	0.382	0.021
3.85	(3)	$(\frac{7}{2}^-)$	1.50	0.078
4.03	(1)	$(\frac{3}{2}^-)$	3.60	0.24
4.20	(3)	$(\frac{3}{2}^-)$	1.57	0.071
4.55			0.699	
4.67			1.16	
4.73			2.50	
4.83	(3)	$(\frac{7}{2}^-)$	1.77	0.059

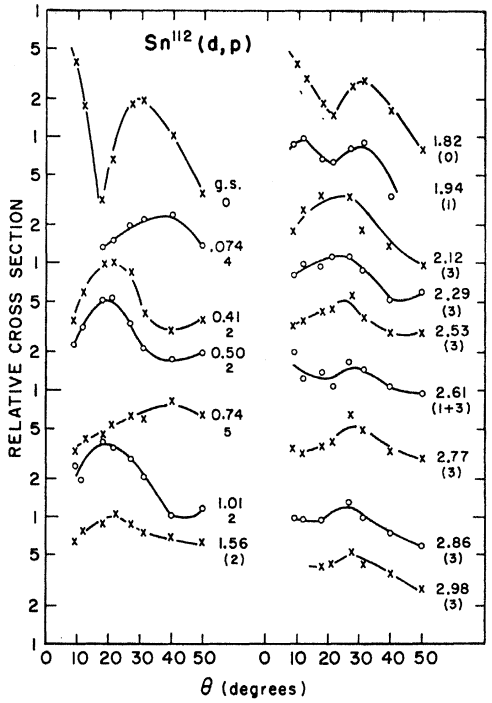

FIG. 3. Angular distributions for the proton groups leading to the states of Sn^{113}. Smooth curves are drawn through the experimental points to aid the reader. The numbers to the right of the angular distributions are the excitation energies and the values of the orbital angular momentum of the captured neutron. If the distribution is fit with more than one value of orbital angular momentum, it is indicated by a+ sign between the orbital angular momenta noted. Tentative assignments are listed in parentheses.

cross section calculated using the DWBA (JULIE) program.[4]

The (d,p) angular distributions for the levels of the even-odd isotopes are shown in Fig. 3–9. They are labeled by the energy and the assigned value of l_n. The lines drawn through the experimental points do not represent any theoretically predicted angular distributions but only serve to aid the reader.

The values of l_n were found by comparing the experimental angular distributions with the calculated angular distributions from distorted-wave theory. The DWBA calculations were done on the University of Pittsburgh IBM 7090 computer[4] using the Oak Ridge Code JULIE of Bassel, Drisko, and Satchler. The optical-model parameters were chosen from fits to elastic scattering data[5] and include spin-orbit potentials for the neutron and proton channels. Comparisons between experimental and calculated angular distributions are shown in Fig. 10–15 inclusive. These figures include the experimental angular distributions and two types of calculated DWBA angular distributions—one with, and the other without a lower radial cutoff (LCO) in the integration of the form factor integral. The fits to the experimental data, especially for $l_n=0$ (cf. Fig. 10), were better if a lower cutoff is used in the calculations. The calculations with the lower cutoffs were therefore used in the analysis of the data. The angular distributions for the $d_{3/2}$ and $d_{5/2}$ single-particle states differ only in magnitude; the $d_{5/2}$ calculated cross section is approximately 15% larger than the $d_{3/2}$ cross section.

For the peaks which contain more than one level, DWBA angular distributions were added together in an attempt to fit the observed angular distribution and the two l_n values are given. In the case of $Sn^{114}(d,p)$, the angular distributions of two peaks were known to contain contributions from $Sn^{116}(d,p)$. For these cases, the experimentally known angular distributions from the latter reaction were used in conjunction with the DWBA angular distributions in order to obtain a fit to the angular distribution for the observed peak. Figure 16 shows the experimental angular distribution for the 0.72-MeV

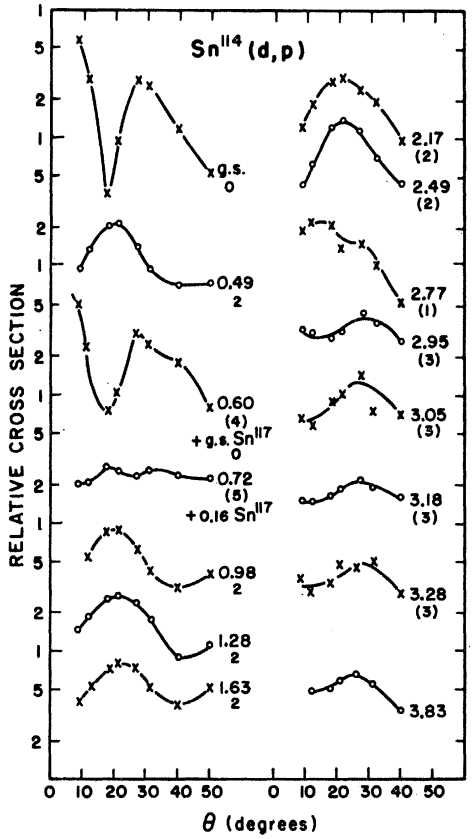

FIG. 4. Angular distributions for the proton groups leading to the state of Sn^{115}. See also caption for Fig. 3.

[4] The calculations reported in this study were performed at the University of Pittsburgh computation center which is partially supported by the National Science Foundation under Grant No. G-11309. The DWBA program was developed and supplied to the authors by R. Bassel, R. M. Drisko, and G. R. Satchler.

[5] C. M. Perey and F. G. Perey, Phys. Rev. 132, 755 (1963); F. G. Perey, *ibid.* 131, 745 (1963). The optical-model parameters used are: Deuterons: $V_0=97.2$ MeV, $r_0=1.15$ F, $r_{0c}=1.115$ F, $a=0.81$ F, $r_0'=1.34$ F, $a'=0.68$ F, and $W'=64$ MeV. Protons: $V_0=49$ MeV, $r_0=1.25$ F, $r_{0c}=1.25$ F, $a=0.65$ F, $r_0'=1.25$ F, $a'=0.47$ F, $W'=54.4$ MeV, and $V_{so}=7.5$ MeV. The potentials were Woods-Saxon with surface derivative absorption.

peak along with the two angular distributions used to fit the experimental distribution.

The ground-state transitions for Sn^{113}, Sn^{115}, Sn^{117}, and Sn^{119} have $l_n=0$ angular distributions and are thus assigned to be $\frac{1}{2}^+$. For the heavier tin isotopes, Sn^{121}, Sn^{123}, and Sn^{125}, the ground state and first excited states

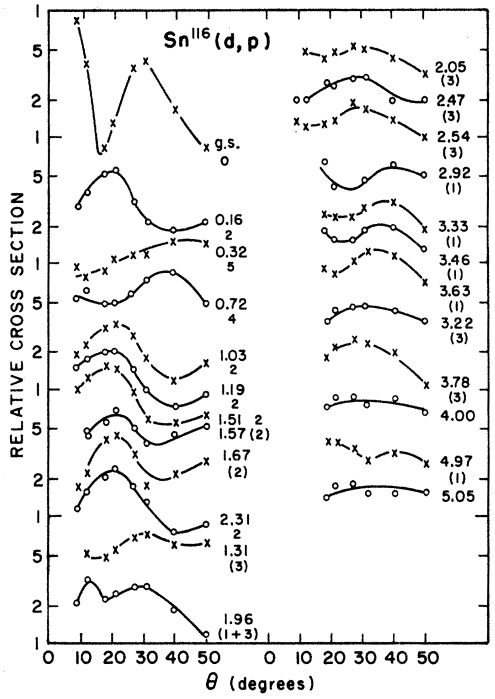

FIG. 5. Angular distributions for the proton groups leading to the states of Sn^{117}. See also caption for Fig. 3.

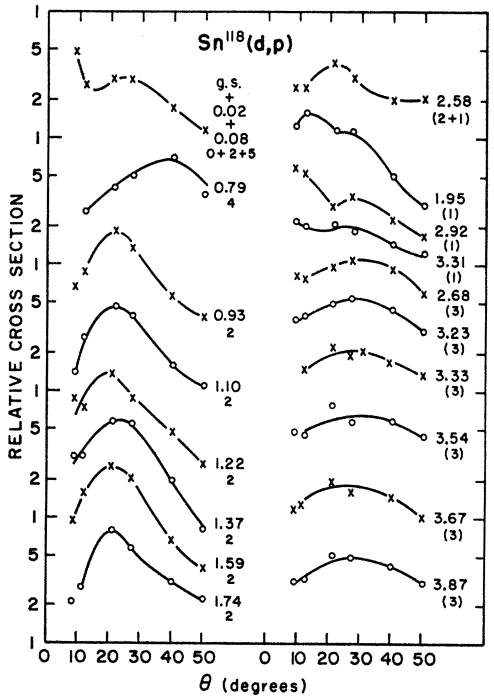

FIG. 6. Angular distributions for the proton groups leading to the states of Sn^{119}. See also caption for Fig. 3.

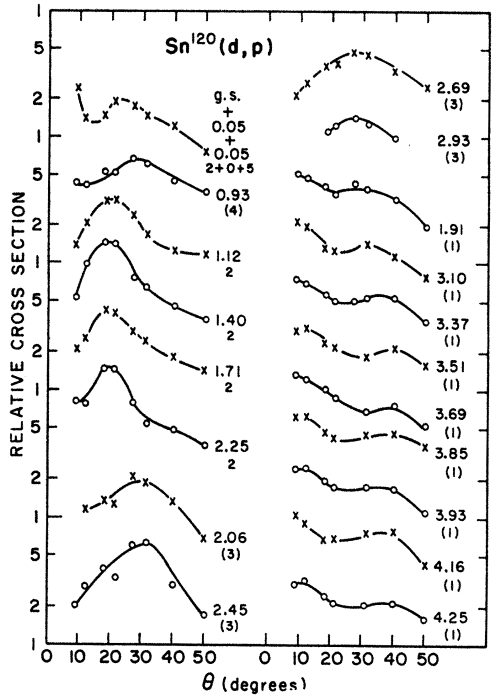

FIG. 7. Angular distributions for the proton groups leading to the states of Sn^{121}. See also caption for Fig. 3.

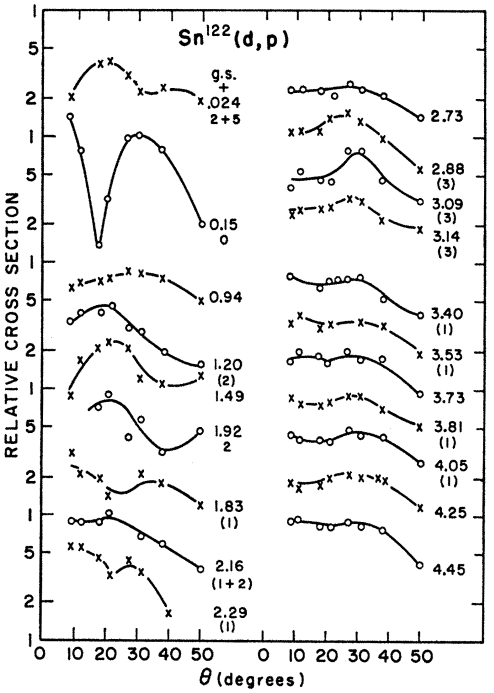

FIG. 8. Angular distributions for the proton groups leading to the states of Sn^{123}. See also caption for Fig. 3.

are very close in energy and could not be resolved in our study. In Sn^{121}, the $\frac{3}{2}^+$ ground state and the $\frac{1}{2}^+$ and $11/2^-$ excited states are all within 60 keV of each other, so that the observed angular distribution contains $l_n=0$, 2, and 5. In the case of Sn^{123} and Sn^{125}, the ground state and the first excited state are separated by ~25 keV. The situation in these two cases has been clarified by the work of Sheline and Nealy.[6] They resolved the two states and identified the ground state to be $11/2^-$ and the first excited state to be $\frac{3}{2}^+$. Since the latter is much more strongly excited than the ground state, the strong peak observed in this study is that due to the first excited state.

In $Sn^{114}(d,p)Sn^{115}$, the proton groups from the 0.60- and the 0.72-MeV levels were contaminated by protons from $Sn^{116}(d,p)$. After the angular distributions for the latter were subtracted from the observed experimental angular distributions, the resultant angular distributions could be assigned either $l_n=4$ or $l_n=5$. As may be seen in Fig. 16, the fit to the 0.72-MeV peak was better if an $l_n=5$ angular distribution was added to the $l_n=2$ angular distribution from the Sn^{116} contaminant. The assignments for these two states was also influenced by the following argument. In the light isotopes of tin, the $g_{7/2}$ state is almost full whereas the $h_{11/2}$ is almost completely empty. Therefore, the ratio of the (d,p) to the (d,t) cross sections for exciting an $h_{11/2}$ state should be much larger than that ratio for exciting a $g_{7/2}$ state. From

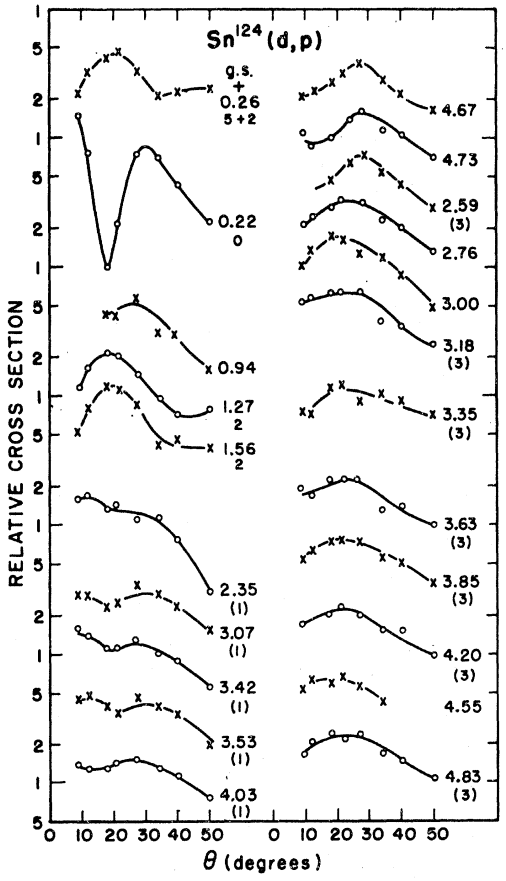

FIG. 9. Angular distributions for the proton groups leading to the states of Sn^{125}. See also caption for Fig. 3.

[6] C. L. Nealy and R. K. Sheline, Phys. Rev. 135, B325 (1964).

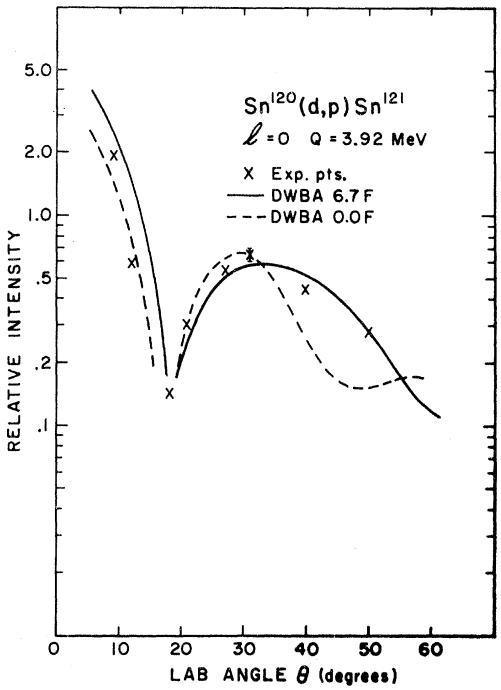

FIG. 10. An example of an experimental angular distribution for a $l_n=0$ transition compared with the DWBA prediction. The calculated curves are given for two cases: without any lower cutoff in the calculation 0.0 F, and with the lower cutoff, 6.7 F, which is used in obtaining spectroscopic factors.

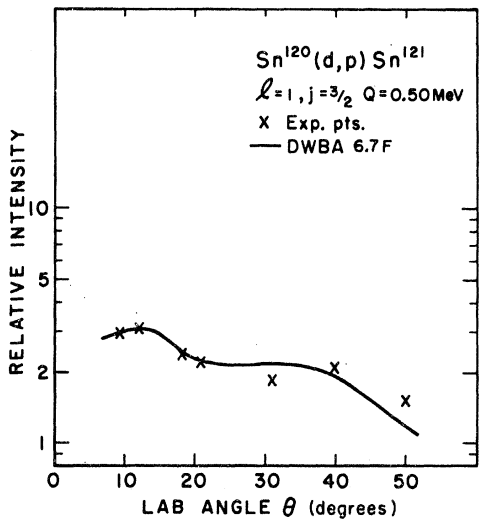

FIG. 11. An example of an experimental angular distribution for a $l_n=1$ transition compared with the DWBA prediction. The calculated curve with a lower cutoff of 6.7 F is given.

Table II, this ratio is 0.57 for the 0.60-MeV state, while it is 6.7 for the 0.72-MeV state. This very strongly suggests that the former is $\frac{7}{2}^+$ while the latter is $11/2^-$.

The $11/2^-$ state could only be clearly resolved in the cases of Sn^{113} and Sn^{117}. In the other isotopes, the $11/2^-$ level was masked either by an isotopic impurity or by strong, nearby peaks of the same isotopes. This problem is complicated by the fact that cross sections for the

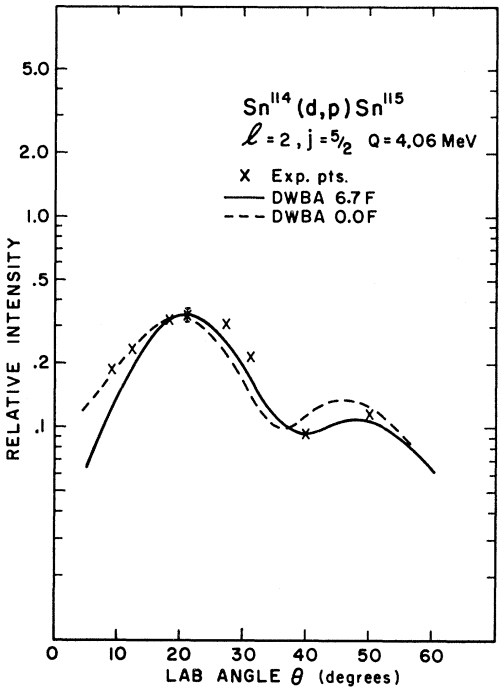

FIG. 12. An example of an experimental angular distribution for a $l_n=2$ transition compared with the DWBA prediction. See also caption for Fig. 10.

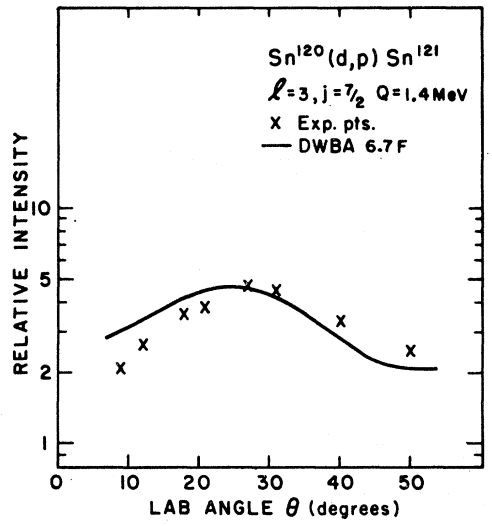

FIG. 13. An example of an experimental angular distribution for a $l_n=3$ transition compared with the DWBA prediction. See also caption for Fig. 11.

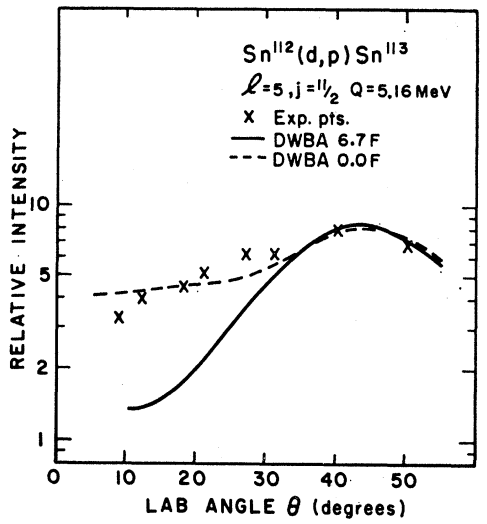

FIG. 14. An example of an experimental angular distribution for a $l_n=4$ transition compared with the DWBA prediction. See also caption for Fig. 10.

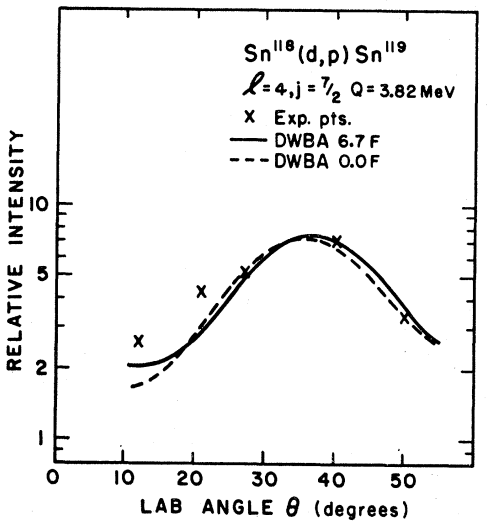

FIG. 15. An example of an experimental angular distribution for a $l_n=5$ transition compared with the DWBA prediction. See also caption for Fig. 10.

$11/2^-$ state were generally much smaller than the cross sections of the contaminants, so a small error in subtracting the contribution from the contaminant peak could easily result in a large error in the cross section for the $11/2^-$ state. Improved resolution would be needed in order to eliminate such a problem.

For the levels which are assigned $l_n=2$, there is an ambiguity in the final spin between $j=\frac{5}{2}$ and $j=\frac{3}{2}$. In the lighter tin isotopes, the $d_{5/2}$ shell-model state is almost full while the $d_{3/2}$ state is relatively empty; so the ratio $\sigma(d,p)/\sigma(d,t)$ for the reactions leading to the same level should be very much smaller for $d_{5/2}$ than for $d_{3/2}$ states. Striking differences were indeed found in many cases, allowing definite assignments to be made.

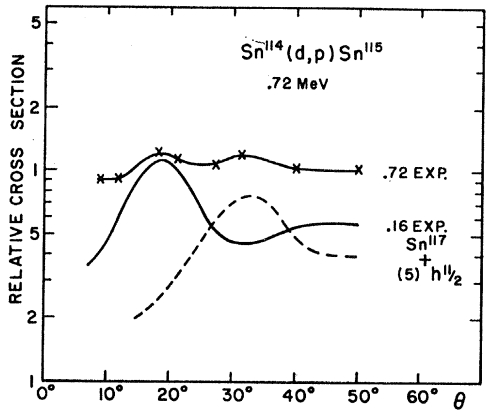

FIG. 16. The experimental angular distribution for the 0.72-MeV level of Sn^{115} which contains the 0.16-MeV $d_{3/2}$ level of Sn^{117}. The properly normalized experimental $d_{3/2}$ angular distribution is subtracted from the observed distribution. The resulting angular distribution (dashed curve) is that of a $l_n=4$ or 5 distribution. See also text.

However, some of the more highly excited states could not be studied with the (d,t) reaction, so this method could not be used. In such cases, levels are tentatively assigned as $\frac{5}{2}^+$, since $\frac{3}{2}^+$ states are generally expected at much lower energies. While a few of these assignments may be in error, the intensities of these levels are small and do not greatly influence the results in the next section.

In the previous paper of Cohen and Price,[1] the low-lying state at approximately 0.9 MeV in the heavier isotopes was described as a non-single-particle state. In Sn^{119}, this state appears to have an $l_n=2$ angular distribution and is tentatively assigned to be a $\frac{5}{2}^+$ state. In Sn^{121}, this state appears to have a $l_n=4$ angular distribution and is assigned as a possible $\frac{7}{2}^+$. The cross section for exciting this in Sn^{121} by the (d,t) reaction is consistent with the expected cross section for a $\frac{7}{2}^+$ state. In Sn^{123} and Sn^{125}, the angular distributions for the ~0.9 MeV state are peaked at an angle greater than that expected for an $l_n=2$ transition, and the cross section for exciting them by the (d,p) reaction is very similar to that found in Sn^{121}; however, the cross section for exciting the state in Sn^{123} by the (d,t) reaction is almost an order of magnitude smaller than in Sn^{121}. This seems to support the conclusion of Cohen and Price that the state is a non-single-particle state in Sn^{123} and Sn^{125}. No $\frac{7}{2}^+$ states were observed in Sn^{123} and Sn^{125} but these states are weakly excited and could easily be masked by nearby levels.

Many states with $l_n=1$ and $l_n=3$ were observed at higher excitation energies. The states in this region of excitation are dense and it is possible to identify only the stronger ones. In this region of excitation energies, the Q value is very low and the angular distributions are relatively flat and structureless, so that assignments are not often certain. These states belong to the next major shell (83–126 neutrons) and are tentatively assigned to the lowest $l=1$ and $l=3$ shell-model states of that shell, the $p_{3/2}$ and $f_{7/2}$ states.

TABLE VIII. The sum of the spectroscopic factors of the shell-model states from the (d,p) reaction on the even-even isotopes of tin.

Shell-model state	112	114	116	118	120	122	124
$s_{1/2}$	1.16	0.96	0.65	0.59	0.39	0.37	0.26
$d_{3/2}$	0.75	0.62	0.55	0.52	0.43	0.43	0.34
$d_{5/2}$	0.22	0.23	0.14	0.16	0.12	0.09	0.06
$g_{7/2}$	0.31	0.19	0.13	0.14	0.19		
$h_{11/2}$	1.00	0.77	0.81	0.56			

IV. COMPARISON OF RESULTS WITH THEORETICAL PREDICTION

In Tables I–VII, spectroscopic factors are listed for the (d,p) reaction. The sum $\sum_m S^m(j)$ of these spectroscopic factors of all nuclear levels of shell-model state j is the "emptiness," U_j^2, of the state. The sums of the experimental spectroscopic factors are listed in Table VIII.

Likewise, from the (d,t) experimental cross section, the "fullness," V_j^2, can be obtained. The (d,t) experimental cross section can be expressed as

$$\frac{d\sigma}{d\Omega}(d,t)=T(l_n,\theta,Q)S(d,t) \tag{2}$$

for an even target. The function $T(l_n,\theta,Q)$ is the single-particle cross section which can be calculated by DWBA. However, good triton optical-model parameters are not presently available for the tin isotopes. If we assume that Q dependence of $T(l_n,\theta,Q)$ can be separated out as

$$T(l_n,\theta,Q)=T'(l_n,\theta)A^Q, \tag{3}$$

the value of A can be determined from DWBA calculations.

For (d,t) reactions on an even-even nucleus, the fullness V_j^2 can be written

$$V_j^2=\frac{1}{2j+1}\sum_m S_j^m(d,t)\cdot \tag{4}$$

Since T' is the same for all levels of the same j, substitution of (2) and (3) into (4) gives

$$V_j^2=\frac{1}{T_j'}\sum_m\left[\frac{(d\sigma/d\Omega)_m}{Q_m}\right]. \tag{5}$$

The summation may be determined from the experimental data, so that the quantity $T_j'\ V_j^2$ is thereby determined. It is a function of the angle of observation, but this presents no difficulty in the ensuing analysis as long as the same angle is used throughout.

It is well known that absolute cross sections as calculated by DWBA may be in error by normalization

factors differing from unity by as much as 30%. Since data have been obtained here on a large number of isotopes, and since there are independent determinations of U_j^2 and V_j^2 whereas these two quantities are related by

$$U_j^2+V_j^2=1, \tag{6}$$

there is a redundancy of data which can be used to determine these normalization factors. This was done by imposing the condition that the sum of U_j^2 and V_j^2 must vary in a regular monotonic fashion with isotopic mass.

The procedure was to form the sum

$$\alpha_j U_j^2+T_j' V_j^2=B_j \tag{7}$$

for each isotope. The U_j^2 and $T_j'V_j^2$ are taken from the experimental data as described above, and α_j determined by imposing the condition that B_j does not vary monotonically with isotope mass. Once α_j is determined in this way, B_j is determined from (7), and its average over the various isotopes, $\bar{B}_j$, is readily determined. If the normalized U_j^2 and V_j^2 are designated $U_j'^2$ and $V_j'^2$, respectively, the condition (6) gives

$$\begin{aligned} U_j'^2&=(\alpha_j/B_j)U_j^2, \\ V_j'^2&=(T'/B_j)V_j^2. \end{aligned} \tag{8}$$

The normalization factors α_j/B_j are listed in Table IX; it should be noted that they do not differ from unity by more then the expected 30%. The values of $U_j'^2$ and $V_j'^2$ are listed in Table X; they will henceforth be treated as unprimed values of U_j^2 and V_j^2.

The experimental spectroscopic factors were not used to obtain $U_{11/2}^2$ and $V_{11/2}^2$ because of the difficulty in obtaining reliable absolute cross sections for these states. Since the V_j^2 describe the fullness of a given shell-model state,

$$\sum_j (2j+1)V_j^2=n, \tag{9}$$

where n is the number of neutrons an isotope has outside the last closed neutron shell which in the case of tin is at 50 neutrons. The values of $V_{11/2}^2$ were determined from[7] using the known values of V_j^2 for the other states.

Plots of the average between the U_j^2 and $(1-V_j^2)$ versus isotopic mass are shown in Fig. 17. These plots show the expected behavior that the shell-model states fill monotonically and simultaneously as neutron pairs are added.

The single quasiparticle energies E_j may also be obtained from the data listed in Tables I–VII inclusive.

TABLE IX. The coefficients of renormalization used in calculating the renormalized occupation numbers.

	Shell-model state			
	$s_{1/2}$	$d_{3/2}$	$d_{5/2}$	$g_{7/2}$
$\alpha_j/\bar{B}_j$	0.76	1.2	1.3	0.99

[7] S. T. Belyaev, Kgl. Danske Videnskab. Selskab, Mat. Fys. Medd. **31**, No. 11 (1959).

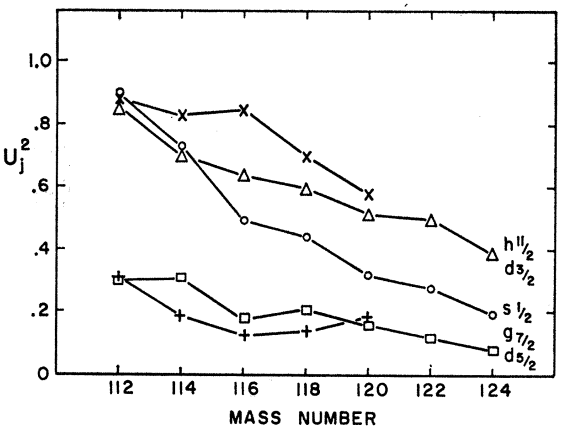

FIG. 17. Plot of the average of the renormalized U_j^2 and $(1-V_j^2)$ as a function of the mass number for the even-even Sn isotopes.

These energies are taken to be the "centers of gravity" of the observed states, weighting each with its spectroscopic factor; thus

$$E_j=\frac{\sum_m E_j^m S_j^m}{\sum_m S_j^m}, \tag{10}$$

where the summation is over all members of a single-particle transition multiplet and E_j^m is the excitation energy for a given level measured relative to the ground state. The quasiparticle energies thus obtained are listed in Table XI. The centers of gravity for the observed $l=1$ and $l=3$ peaks were also found, but it is believed that only a part of the transition strength for these states was observed, so the quasiparticle energies for these cases are higher than the centers of gravity for the observed levels. Figure 18 shows the plot of the quasiparticle energies for the states of the 50–82 neutron shell versus the mass of the isotope.

According to the giant resonance theory of Lane, Thomas, and Wigner[8] the width of the energy distribution of the levels belonging to a shell-model state should

TABLE X. The renormalized occupation numbers for the even isotopes of tin. The method is described in Sec. IV.

		Mass numbers						
		112	114	116	118	120	122	124
$s_{1/2}$	$U_{1/2}^2$	0.89	0.73	0.49	0.45	0.30	0.28	0.19
	$V_{1/2}^2$		0.26	0.52	0.64		0.73	0.80
$d_{3/2}$	$U_{3/2}^2$	0.86	0.72	0.64	0.60	0.50	0.50	0.39
	$V_{3/2}^2$		0.31	0.32	0.38		0.51	0.69
$d_{5/2}$	$U_{5/2}^2$	0.30	0.31	0.18	0.21	0.16	0.12	0.08
	$V_{7/2}^2$		0.60	0.81	0.82	0.94	0.86	0.94
$g_{7/2}$	$U_{7/2}^2$	0.31	0.19	0.13	0.14	0.19		
	$V_{7/2}^2$		0.86	0.88	0.81	0.70		
$h_{11/2}$[a]	$U_{11/2}^2$	0.88	0.83	0.85	0.70	0.58		
	$V_{11/2}^2$	0.12	0.17	0.15	0.30	0.42		

[a] The values are chosen to satisfy relation (9).

[8] A. M. Lane, R. G. Thomas, and E. P. Wigner, Phys. Rev. **98**, 693 (1955).

TABLE XI. The single-quasiparticle energies (in MeV) for the shell-model states in the odd isotopes of tin.

l_j	Sn^{113}	Sn^{115}	Sn^{117}	Sn^{119}	Sn^{121}	Sn^{123}	Sn^{125}
$s_{1/2}$	0.13	0.24	0	0	0.05	0.22	0.29
$d_{3/2}$	0.50	0.49	0.16	0.024	0	0.024	0.026
$d_{5/2}$	0.73	1.37	1.30	1.43	1.45	1.31	1.38
$g_{7/2}$	0.074	0.60	0.72	0.79	0.93		
$h_{11/2}$	0.74	0.72	0.32	0.08	0.05	0	0
$p_{3/2}$	>3.00	>3.80	≥3.97	>3.00	≥3.63	≥3.70	≥3.84
$f_{7/2}$	>3.00	≥3.50	≥3.35	≥3.42	≥2.70	≥2.90	≥3.23

be $2W$, where W is the depth of the imaginary optical-model potential. In Ref. 3, evidence was presented that the W for a bound state is approximately $\frac{1}{3}E^*$, where E^* is the excitation energy for the shell-model state and is taken to be the single-quasiparticle energy. Figure 19

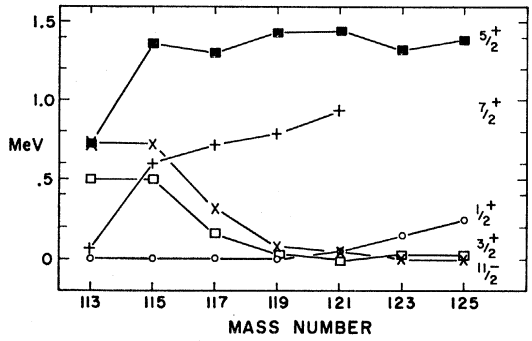

FIG. 18. The centers of gravity of the single-quasiparticle states in the $50<N<82$ neutron shell are plotted against the mass number.

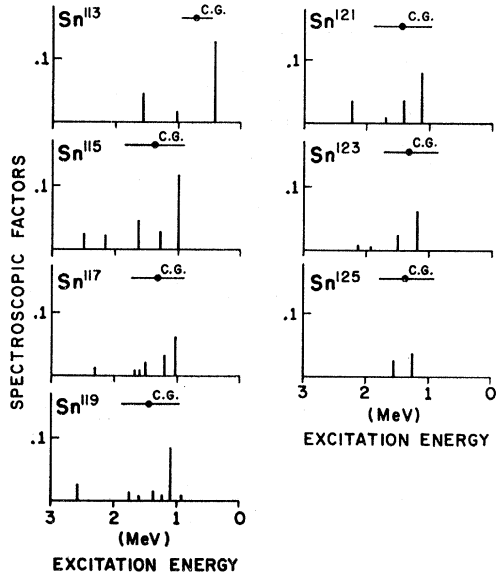

FIG. 19. The energy distribution of the levels belonging to the $d_{5/2}$ state in each nucleus and their centers of gravity. The height of each line is proportional to the spectroscopic factor for each level. The solid circles designate the centers of gravity of the levels; the horizontal bars centered on the solid circles designate the width of the single-particle levels expected from the giant resonance theory of Lane, Thomas, and Wigner (Ref. 8).

shows the energy distributions of the levels assigned to the $d_{5/2}$ state and their respective centers of gravity. The heights of the lines are porportional to the spectroscopic factors for these levels. The horizontal bars in the figure show the widths expected from the prescription. The agreement between the two is reasonably good.

Pairing theory[7,9] gives a relation between the occupation numbers (U_j^2, V_j^2) and the single-particle energies ϵ_j of the shell model as

$$U_j^2=\tfrac{1}{2}\left\{1+\frac{(\epsilon_j-\lambda)}{[(\epsilon_j-\lambda)^2+\Delta^2]^{1/2}}\right\}, \tag{11}$$

$$V_j^2=\tfrac{1}{2}\left\{1-\frac{(E_j-\lambda)}{[(E_j-\lambda)^2+\Delta^2]^{1/2}}\right\}, \tag{12}$$

where λ is the energy of the Fermi surface and Δ is half the "energy gap". Using (11) and (12), and explicit expression for $(\epsilon_j-\lambda)$ may be obtained[1]:

$$(\epsilon_j-\lambda)=\Delta\left[\frac{U_j^2-V_j^2}{2(U_j^2V_j^2)^{1/2}}\right]. \tag{13}$$

Pairing theory also provides a simple relation between the quasiparticle energies and the single-particle energies,[1]

$$E_j=\Delta\left[1+\left(\frac{\epsilon_j-\lambda}{\Delta}\right)^2\right]^{1/2}. \tag{14}$$

From relation (14) another expression for $(\epsilon_j-\lambda)$ can be obtained.

$$(\epsilon_j-\lambda)=\pm\Delta\left[\left(\frac{E_j}{\Delta}+1\right)^2-1\right]^{1/2}. \tag{15}$$

Using the expressions (13) and (15) and the experimentally determined values for the occuaption numbers and single-quasiparticle energies, relative single-particle energies $(\epsilon_j-\epsilon_{5/2})$ may be obtained. The single-particle

TABLE XII. Values of Δ used in calculating the single-particle energies.

	112	114	116	118	120	122	124
Δ (MeV)	1.15	1.19	1.25	1.40	1.49	1.50	1.44

[9] L. S. Kisslinger and R. A. Sorensen, Kgl. Danske Videnskab. Selskab, Mat. Fys. Medd. **32**, No. 9 (1960).

TABLE XIII. The single-particle energies (in MeV) for the even isotopes of tin measured relative to the energy of the $d_{5/2}$ state. These energies are calculated using the renormalized occupation numbers (U_j^2) and also from the quasiparticle energies (E_j).

Single-particle energies		Mass number 112	114	116	118	120	122	124
$(\epsilon_{1/2}-\epsilon_{5/2})$	(U_j^2)	1.93	1.05	1.03	1.01	0.85	0.98	1.14
	(E_j)		1.90	2.29	2.39	2.33	1.92	1.63
$(\epsilon_{3/2}-\epsilon_{5/2})$	(U_j^2)	1.70	0.93	1.45	1.35	1.50	1.72	1.24
	(E_j)		3.10	3.26	2.87	2.65	2.31	2.13
$(\epsilon_{7/2}-\epsilon_{5/2})$	(U_j^2)	0.29	−0.60	−0.35	−0.36	+0.46		
	(E_j)		1.00	0.83	0.75	0.70		
$(\epsilon_{11/2}-\epsilon_{5/2})$	(U_j^2)	1.85	1.50	2.26	1.64	1.58		
	(E_j)		3.40	3.53	3.15	2.98	2.70	2.39

energies calculated using (13) are those for the even isotopes and the values obtained using (15) are for the odd isotopes. In order to compare the values obtained using the quasiparticle energies with the value determined from the occupation numbers, an interpolation was made between adjacent masses. The value of Δ was determined from the separation energies (SE) using the relation

$$\Delta(n)=\tfrac{1}{4}\times\{|\mathrm{SE}(n)-\mathrm{SE}(n-1)|+|\mathrm{SE}(n)-\mathrm{SE}(n+1)|\}. \quad (16)$$

The separation energies were obtained from the studies of Ries, Damerow, and Johnson[10] and Cohen, Patell, Prakash, and Schneid.[11] The values of Δ used are tabulated in Table XII. The relative single-particle energies are tabulated in Table XIII.

The relative single-particle energies calculated using the single-quasiparticle energies are approximately a factor of 2 greater than the energies calculated using the occupation numbers. These single-particle energies are measured relative to the single-particle energies for the $d_{5/2}$ state. The occupation numbers and single-quasiparticle energies for this state may be slightly in error because of incorrect assignment of final spins for the weak, high-lying $l=2$ states. This could result in an error to the single-particle energies of approximately ± 0.3 MeV. The errors in the experimental data are not large enough to account for the differences in relative single-particle energies. The relative single-particle energies calculated from the experimental quasiparticle energies show a dependence on the mass of the isotopes, whereas the relative single-particle energies determined from the occupation numbers are almost constant as the mass increases. The single-particle energies are not expected to vary greatly as the mass of the isotope changes, so the energies derived from the occupation numbers are better in this respect.

In Table XIV the values of the single-particle energies are compared to the values previously obtained by Cohen and Price,[1] and to the values given by Kisslinger and Sorensen.[12] The energies of Cohen and Price were obtained using a value for Δ equal to 1.1 MeV taken from a previous work of Kisslinger and Sorensen.[9]

The single-particle energies calculated with the occupation numbers should be more reliable than those calculated from the quasiparticle energies since the latter are influenced by the long-range forces (such as

TABLE XIV. Comparison of the relative single-particle energies (in MeV) between this paper, Cohen and Price (Ref. 1) and Kisslinger and Sorensen (Ref. 12). The experimental relative single energies are calculated using the renormalized occupation numbers (U_j^2) and the quasiparticle energies (E_j).

		Mass number 116			118			120			122			124		
		S-P-C	K-S	C-P	S-P-C	K-S	C-P	S-P-C	K-S	C-P	S-P-C	K-S	C-P	S-P-C	K-S	C-P
$(\epsilon_{1/2}-\epsilon_{5/2})$	(V_j^2)	1.03	1.32	0.97	1.01	1.32	0.83	0.85	1.30	0.97	0.98	1.28	0.70	1.14	1.28	1.24
	(E_j)	2.29		1.65	2.39		1.72	2.33		1.57	1.92		1.40	1.63		1.37
$(\epsilon_{3/2}-\epsilon_{5/2})$	(V_j^2)	1.45	2.86	1.44	1.35	2.84	1.22	1.50	2.80	1.10	1.72	2.76	0.96	1.84	2.75	1.41
	(E_j)	3.26		2.45	2.87		2.12	2.65		1.87	2.13		1.85	2.13		1.94
$(\epsilon_{7/2}-\epsilon_{5/2})$	(V_j^2)	−0.35	0.84	0.08	−0.36	0.82	−0.33	+0.46	0.80	−0.22		0.77			0.77	
	(E_j)	0.83		0.42	0.75		0.37	0.70		0.22						
$(\epsilon_{11/2}-\epsilon_{5/2})$	(V_j^2)	2.26	2.51	1.34	1.64	2.51	1.22	1.58	2.50	1.54		2.48	1.22		2.47	1.75
	(E_j)	3.53		2.75	3.15		2.32	2.98		2.12	2.70		2.05	2.39		1.94

[10] R. R. Ries, R. A. Damerow, and W. H. Johnson, Jr., Phys. Rev. **132**, 1662 (1963).
[11] B. L. Cohen, R. Patell, A. Prakash, and E. J. Schneid, Phys. Rev. **135**, B383 (1964).
[12] L. S. Kisslinger and R. A. Sorensen, Rev. Mod. Phys. **35**, 853 (1963).

TABLE XV. Relative single-particle energies (in MeV) calculated with the experimental quasiparticle energies (a) and the energies calculated with quasiparticle energies that were corrected for the magnitude of quadrupole interaction (b).

		Mass number			
		114	116	118	120
$(\epsilon_{1/2}-\epsilon_{5/2})$	(a)	1.90	2.28	2.39	1.33
	(b)	2.00	2.55	2.55	2.36
$(\epsilon_{3/2}-\epsilon_{5/2})$	(a)	3.10	3.26	2.87	2.65
	(b)	3.50	3.38	3.10	3.10
$(\epsilon_{7/2}-\epsilon_{5/2})$	(a)	1.00	0.83	0.75	0.70
	(b)	1.45	1.25	1.29	0.128
$(\epsilon_{11/2}-\epsilon_{5/2})$	(a)	3.40	3.53	3.15	2.98
	(b)	3.21	3.23	3.27	3.31

the quadrupole force) whereas these forces do not influence the occupation numbers.

Kisslinger and Sorensen[12] have calculated the quasiparticle energies both with and without the quadrupole interaction. The principal contribution of this interaction is to lower the $d_{5/2}$ state in the heavier isotopes. It also keeps the $s_{1/2}$ state as the ground state or low-lying level and lowers the $d_{3/2}$ state below the $h_{11/2}$ state in the heavier isotopes. In the last case, it is found that the $h_{11/2}$ state is the ground state for the heavier isotopes—not the $d_{3/2}$ state.

Using the calculated magnitude of the energy shift for these levels in the presence of the quadrupole interaction, the experimental quasiparticle energies can be corrected for the quadrupole interaction and the relative single-particle energies can be recalculated. These energies listed in Table XV, do not give better agreement with the energies obtained from the occupation numbers, but the values of the single-particle energies do not show as great a dependence on the mass number as before.

TABLE XVI. Comparison between Yoshida's (Ref. 8) predicted energies and transition strengths for the $\frac{5}{2}^+$ states and the experimental energies and transition strengths.

Yoshida		Expt	
E^* (MeV)	$G(d,p)$	E^* (MeV)	$d\sigma/d\Omega$ $(2j+1)S$
	Sn^{113}		
0.12	1.2	0.41	0.9
1.19	0.15	1.01	0.1
1.54	0.002	1.56	0.3
	Sn^{115}		
0.54	0.72	0.98	0.7
1.25	0.051	1.28	0.2
1.46	0.009	1.63	0.2
		2.17	0.1
		2.49	0.1
	Sn^{117}		
0.74	0.53	1.03	0.4
1.34	0.057	1.19	0.2
1.40	0.00096	1.51	0.1
		1.59	0.04
		1.67	0.04
		2.31	0.07
	Sn^{119}		
0.78	0.39	0.93	0.04
1.25	0.007	1.10	0.5
1.53	0.015	1.22	0.06
		1.37	0.08
		1.59	0.04
		1.74	0.06
		2.58	0.2
	Sn^{121}		
0.80	0.28	1.12	0.4
1.20	0.004	1.40	0.2
1.60	0.043	1.71	0.02
		2.25	0.2

Yoshida[13] has made a spectroscopic study of low-energy vibrational states of spherical nuclei and predicted the energies and the transition rates for (d,p) and (d,t) reactions for various states in the isotopes of tin. In a few cases, he predicts previously unknown levels with transition rates large enough to be detected in these experiments. In the case of Sn^{117}, Yoshida predicts a $s_{1/2}$ level at 1.37 MeV with an intensity approximately 15% that of the ground-state transition; no evidence was found for any $l_n=0$ level in Sn^{117} other than the ground state. Likewise, he predicts an $l_n=0$ level in Sn^{119} at 1.26 MeV which should be observed, but again there is no evidence for such a level.

In Sn^{117}, Yoshida finds that the $h_{11/2}$ state is divided into two levels, at 0.27 and 1.67 MeV, with the latter having about $\frac{1}{4}$ of the transition strength. Again there is no evidence for such a level, although it could be masked if it is sufficiently near another strong level in this energy region.

TABLE XVII. Results for Sn^{114}.

$E(d,t)$ (MeV)	J^π	(d,t) $d\sigma/d\Omega(45°)$ (mb/sr)	$E(d,d')$[a] (MeV)	(d,d') Parity
0	0^+	1.14		
1.31	2^+	0.331	1.30	+
1.58	0^+	~0.06		
1.95	0^+	0.180	1.97	
2.20		0.260	2.18	
			2.27	−
2.42		0.079		
2.55		0.198		
2.68		0.059		
2.84		~0.04	2.82	−
			2.87	−

[a] Reference 14.

Yoshida also gives the intensities of the (d,p) and (d,t) reactions leaving the residual nucleus in $\frac{5}{2}^+$ states. Table XVI gives his results along with results obtained in this study. It should be noted that the lowest predicted $\frac{5}{2}^+$ state is always lower than the lowest experimental level. Another point to be noted is that these are not all the predicted $\frac{5}{2}^+$ states, but only the lowest three states which carry most of the strength of this level. In fact, the lowest predicted level carries just about all the strength, whereas in the experimental case the strength is found to be distributed among the observed levels.

V. RESULTS OF (d,p) AND (d,t) REACTIONS ON ODD TARGETS

The experimental results for (d,p) and (d,t) reactions on the odd-mass isotopes of tin are summarized in Table XVII–XX, respectively. These tables list the

[13] S. Yoshida, Nucl. Phys. 38, 380 (1962).

TABLE XVIII. Results for Sn^{116}.

$E(d,p)$ (MeV)	(d,p) l_n	(d,p) J^π	$(d\sigma/d\Omega)_{max}$ (mb/sr)	S'	(d,t) $E(d,t)$ (MeV)	(d,t) $d\sigma/d\Omega(45°)$	(p,p′) $E(p,p')$[a] (MeV)	(p,p′) J^π	β′ $E(\beta^-)$[b] (MeV)	β′ J^π
0	0	0^+	0.790	0.54	0	1.26				
1.28	2	2^+	0.329	0.27	1.28	0.364	1.291	2^+	1.29	2^+
1.76	0	0^+	0.554	0.29	1.73	0.243	1.762	0^+	1.72	0^+
2.03	0	0^+	0.623	0.32	1.99	0.290				
							2.108	2^+	2.12	2^+
2.23	2	2^+	1.41	0.98	2.18	0.30	2.224	2^+		
							2.267	3^-		
2.37	2	$1^+,2^+,3^+$	0.242	0.16	2.34	0.31	2.366			
							2.391	4^+	2.38	4^+
					2.53	0.68	2.531	4^+	2.53	4^+
2.62	0	0^+	1.62	0.72			2.649			
2.78	2	2^+	2.19	1.37	2.76	0.251	2.803	4^+	2.78	4^+
							2.845			
2.95	2	$1^+,2^+,3^+$	0.405	0.194	2.96	0.184	2.959			
					3.06	0.226	3.047	4^+	3.06	4^+
3.10	...	...	...	...			3.091			
3.17	2	$1^+,2^+,3^+$	0.254	0.116	3.18	0.274				
							3.220			
							3.319			
3.35	2	$1^+,2^+,3^+$	1.50	0.67						
					3.39	0.657	3.423			
							3.468			
					3.55	0.202	3.577			
							3.621			
3.64	2	$1^+,2^+,3^+$	0.961	0.41	3.69	0.629	3.656			
							3.771			
3.80	1	$1^-,2^-$	1.07	0.227	3.83	0.129	3.808			
							3.846			
							3.918			
							3.951			

[a] Reference 15.
[b] Reference 16.

TABLE XIX. Results for Sn^{118}.

$E(d,p)$ (MeV)	(d,p) l_n	(d,p) J^π	$(d\sigma/d\Omega)_{max}$ (mb/sr)	S'	(d,t) $E(d,t)$ (MeV)	(d,t) $d\sigma/d\Omega(45°)$	(p,p′) $E(p.p')$[a] (MeV)	(p,p′) $\frac{1}{2}^\pi$	β′ $E(\beta^-)$[b] (MeV)	β′ J^π
0	0	0^+	1.19	0.70	0	0.946				
1.22	2	2^+	0.489	0.39	1.22	0.289	1.229	2^+	1.228	2^+
1.75	0	0^+	0.207	0.10	1.74	0.135				
2.05	0	0^+	0.178	0.084	2.03	0.192	2.043	0^+	2.04	(2^+)
					2.12	0.026				
							2.278	4^+	2.28	4^+
							2.321	3^-		
2.32	2	$1^+,2^+,3^+$	1.75	1.14	2.30	0.354				
							2.400			
2.49	0	0^+	1.14	0.51	2.47	0.719	2.487	0^+	2.48	(4^+)
2.72	2	2^+	2.32	1.37	2.72	0.416	2.73		2.72	?
									2.77	?
							2.899			
							2.959		2.96	(4^+)
3.06	2	$1^+,2^+,3^+$	0.094	0.042	3.04	0.325				
							3.425			
							3.530			
							3.569			
3.70	2	$1^+,2^+,3^+$	0.283	0.12	3.67	0.359	3.690			
							3.748			
							3.757			
3.79	3	$3^-,4^-$	0.143	0.16	3.80	0.094	3.808			
3.91	2	$1^+,2^+,3^+$	0.494	0.20	3.89	0.306	3.875			
							3.947			
4.04	2	$1^+,2^+,3^+$	0.324	0.13	4.01	0.416				
4.44	2	$1^+,2^+,3^+$	0.222	0.082						

[a] Reference 15.
[b] Reference 16.

TABLE XX. Results for Sn^{120}.

$E(d,p)$ (MeV)	l_n	(d,p) J^π	$d\sigma/d\Omega_{max}$ (mb/sr)	S'	$E(p,p')$[a] (MeV)	(p,p') J^π
0	0	0^+	1.13	0.65		
1.17	2	2^+	0.200	0.15	1.166	2^+
1.88	0	0^+	0.087	0.039	1.872	0^+
					2.088	
2.17	0	0^+	0.055	0.023		
					2.183	4^+
2.31	0	0^+	0.170	0.072	2.272	
					2.346	
					2.391	3^-
2.42	2	$1^+,2^+,3^+$	0.882	0.52		
2.60	0	0^+	0.817	0.32	2.632	0^+
2.73	2	$1^+,2^+,3^+$	0.186	0.11		
2.84	2	$1^+,2^+,3^+$	1.45	0.83	2.830	
					2.919	
2.94	2	$1^+,2^+,3^+$	1.05	0.57	1.963	
					3.169	
3.23	2	$1^+,2^+,3^+$	0.071	0.030	3.223	
					3.266	
					3.445	
3.56	2	$1^+,2^+,3^+$	0.353	0.14	3.540	
					3.574	
					3.646	
3.70	2	$1^+,2^+,3^+$	0.291	0.11	3,710	
					3.777	
					3.811	
3.87	2	$1^+,2^+,3^+$	0.300	0.11	3.860	
					3.926	
					3.986	
4.03	2	$1^+,2^+,3^+$	0.238	0.088		
4.15	2	$1^+,2^+,3^+$	0.527	0.20		

[a] Reference 15.

excitation energies of the levels found in the (d,p) and (d,t) reactions, the values of l_n, the final spins and parities assigned to these levels, the maximum cross sections for the (d,p) reactions, the cross sections for the (d,t) reaction at 45°, and the factor S'. Results from other reactions are listed for comparison. The spectroscopic factor S' equals $[(2J+1)/(2I+1)]S$, and is found in the same manner as described in Sec. II.

The Q values for the (d,t) reaction were such that many of the states reached in the (d,p) reaction could also be studied with the (d,t) reaction. This proved very helpful in the case of $Sn^{115}(d,p)$; since the Sn^{115} target was enriched only to 29%, the proton spectrum contained many isotopic impurities so the energies of the levels of Sn^{116} could only be accurately determined from the (d,t) reaction. The values of l_n and absolute cross sections for the (d,p) reactions were obtained by taking into account the strengths of all the peaks of known isotopic impurities. The method is the same as discussed in Sec. II. In Fig. 20 the energy levels with their spin assignments are plotted for comparison. The spectra are observed to have a great similarity.

Most of the levels observed have either $l_n=0$ or $l_n=2$ angular distributions. The levels formed by coupling a $s_{1/2}$ quasiparticle to the $\frac{1}{2}^+$ ground states of the initial nuclei are assigned as 0^+ since the Pauli exclusion principle does not allow identical $\frac{1}{2}^+$ particles to couple to a spin of 1^+. The levels formed by coupling either $d_{3/2}$ or $d_{5/2}$ particles to the $\frac{1}{2}^+$ ground states are two-quasiparticle states of spins 1^+ and 2^+, and 2^+ and 3^+, respectively. If the final level is 2^+, both the $d_{3/2}$ and $d_{5/2}$ shell-model states can contribute to the cross section. The total cross section for these two-shell model states should be approximately the average of that for exciting the same states in the neighboring odd final nuclei.

No $l_n=4$ angular distributions were observed in this study. It is believed that the $g_{7/2}$ single-particle state is divided among many levels so the cross section to any particular level may be weak and therefore not easily observed.

In Sn^{114}, data are available from the (d,t) reaction on Sn^{115}. In Table XVI, the $Sn^{114}(d,d')$ data of Kim and Cohen[14] are listed for comparison and the agreement of excitation energies is very good. The 3^- state at 2.27 MeV does not appear to be excited by the (d,t) reaction. The ground state and first excited states are known to have spins and parities 0^+ and 2^+, respectively. For assigning spins to the other excited states, use was made of the ratio $\sigma(45°)/\sigma 60°)$ for the (d,t) reaction. From the other even isotopes, it was observed that for ratios greater than two, the value of l_n was zero. Using this method, the assignment of 0^+ was made to the levels at 1.58 and 1.95 MeV.

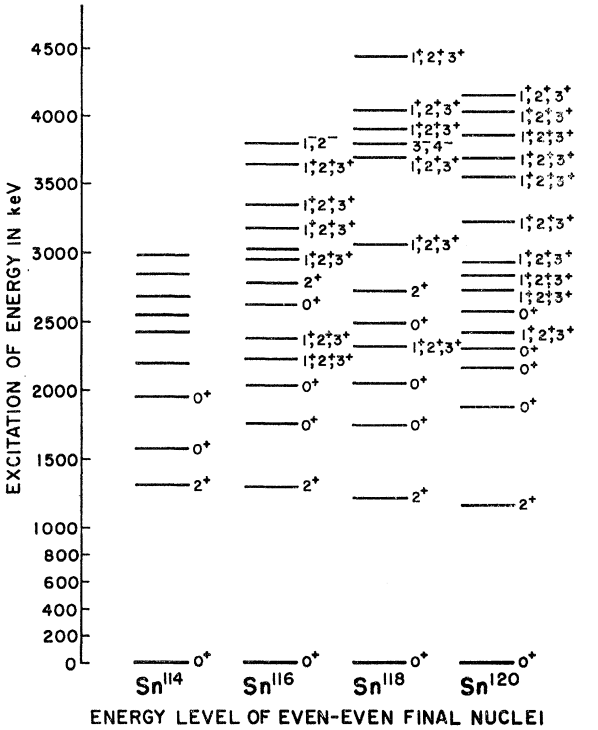

FIG. 20. The energy levels with their respective spin assignments for the even-even nuclei are shown for comparison.

[14] Y. S. Kim and B. L. Cohen, Phys. Rev. 142, 788 (1966).

TABLE XXI. Comparison of the spectra (in MeV) for the data of work done by Norris and Moore (Ref. 17) and the present study. The weak peaks in the data of Norris and Moore are the peaks not seen in this study.

Sn^{118}		Sn^{120}	
N-M	S-P-C	N-M	S-P-C
0	0	0	0
1.22	1.22	1.17	1.17
1.75	1.75	1.88	1.88
2.05	2.05	2.10	
2.32	2.32	2.17	2.17
2.38		2.29	2.31
2.49	2.49	2.36	
2.54		2.43	2.42
2.67		2.61	2.60
2.73	2.72	2.73	2.73
2.81		2.81	
2.84		2.84	2.84
2.86		2.94	2.94
2.89		3.00	
2.92		3.16	
3.05	3.06	3.21	3.23
3.13		3.29	
3.15		3.39	
3.30		3.47	
3.34		3.55	3.56
3.36		3.58	
3.38		3.60	
3.39		3.66	
3.47		3.71	3.70
3.52		3.73	
3.55		3.80	
3.57		3.88	
3.70	3.70	3.94	
3.79	3.79	3.99	
3.89	3.91	4.06	4.03
3.91		4.19	4.15
4.02	4.04	4.35	
4.40	4.44		

In Sn^{116}, there are data from $Sn^{116}(p,p')$ [15] and $In^{116}(\beta^-)$ [16] reactions for comparison. As in Sn^{114}, the 3^- state does not appear to be excited by the (d,p) and (d,t) reaction. There are apparently separate levels at 2.78 MeV (2^+), excited by the $Sn^{115}(d,p)$ reaction and at 2.803 MeV (4^+) excited by the $Sn^{116}(p,p')$ reaction. The 4^+ levels identified in the $Sn^{116}(p,p')$ and $In^{116}(\beta^-)$ reactions at 2.53 and 3.047 MeV may be the same as those seen in the (d,t) reaction, since the (d,t) cross section to a 4^+ state should be strong whereas the (d,p) cross section to the same state should be weak. Only one $l_n=1$ level (at 3.80 MeV) was observed; it is either an 1^- or 2^- state.

In Sn^{118}, data are available from the $Sn^{117}(d,p)$,[17] $Sn^{118}(p,p')$[15], and $In^{118}(\beta^-)$ [16] for comparison. The levels of Sn^{118} were identified by Norris and Moore[17] using the (d,p) reaction, and Table XXI compares the levels found in their study with the levels found in this study; the agreement is very good except for the peaks which are not observed in this study. The level found at 3.06 MeV in the (d,p) reaction and 3.04 MeV in the (d,t) reaction may be two levels. This level strongly excited by the (d,t) reaction and is weakly excited by the (d,p) reaction. It is possible that the (d,t) reaction excites a 3^+ or 4^+ state, whereas the (d,p) reaction excites a 1^+, 2^+, or 3^+ state. This level at 3.79 MeV has an $l_n=3$ angular distribution and is thus either a 3^- or 4^- state.

In Sn^{120}, data are available from the $Sn^{119}(d,p)$ [17] and $Sn^{120}(p,p')$ [15] reaction. The comparison with the (d,p) work of Norris and Moore can be found in Table XXI. As in Sn^{118}, the results agree very well except for the weakly excited states. The 3^- state at 2.91 MeV is very close in energy to the 2.42-MeV state which is either a 1^+, 2^+, or 3^+ state.

ACKNOWLEDGMENTS

The authors are very grateful to R. M. Drisko for his advice and assistance in obtaining DWBA calculations for this study. Thanks are due to R. H. Fulmer and A. L. McCarthy who assisted in the plate exposures; the plate reading group under the direction of Mrs. A. Trent; and the cyclotron operation's group including W. B. Leonard and J. DeFrancesco.

[15] D. L. Allan, B. H. Armitage, and B. A. Doran, Nucl. Phys. **66**, 481 (1965).
[16] H. H. Bolotin, Phys. Rev. **136**, B1557 (1964).
[17] L. R. Norris and C. F. Moore, Phys. Rev. **136**, B40 (1964).